Microfluidic parallel circuit for measurement of hydraulic resistance

Sungyoung Choi, Myung Gwon Lee, and Je-Kyun Park[a)]
Department of Bio and Brain Engineering, College of Life Science and Bioengineering, Korea Advanced Institute of Science and Technology (KAIST), 335 Gwahangno, Yuseong-gu, Daejeon 305-701, Republic of Korea

(Received 30 April 2010; accepted 17 August 2010; published online 31 August 2010)

We present a microfluidic parallel circuit that directly compares the test channel of an unknown hydraulic resistance with the reference channel with a known resistance, thereby measuring the unknown resistance without any measurement setup, such as standard pressure gauges. Many of microfluidic applications require the precise transport of fluid along a channel network with complex patterns. Therefore, it is important to accurately characterize and measure the hydraulic resistance of each channel segment, and determines whether the device principle works well. However, there is no fluidic device that includes features, such as the ability to diagnose microfluidic problems by measuring the hydraulic resistance of a microfluidic component in microscales. To address the above need, we demonstrate a simple strategy to measure an unknown hydraulic resistance, by characterizing the hydraulic resistance of microchannels with different widths and defining an equivalent linear channel of a microchannel with repeated patterns of a sudden contraction and expansion. © *2010 American Institute of Physics.* [doi:10.1063/1.3486609]

I. INTRODUCTION

As microfluidic devices become more common in the fields of biology, chemistry, and nanotechnology, there is an increasing need for standardized modules and off-the-shelf fluidic components. However, unlike microelectronics, in microfluidics there are few standards for microfluidic components, interconnection methods, and control protocols. More importantly, a standard method to measure and characterize microfluidic components and fluidic properties of internal flows has not yet been established.

A multimeter provides a diagnosis of a wide range of electrical problems in wiring systems, power supplies, motor controls, and batteries. Until now, to the best of our knowledge, there is no fluidic counterpart that includes features, such as the ability to diagnose microfluidic problems by measuring the hydraulic resistance of a microfluidic component in microscales. Several efforts have been addressed to measure pressure drop changes by flowing cells and water droplets along a simple comparator microchannel.[1,2] The latter experiment was focused on measuring the hydrodynamic resistance change as well as the pressure drop associated with the motion of a single droplet.[2] In addition, an asymmetric loop network was utilized for measuring the effective hydrodynamic resistance of individual droplets.[3] A conductive elastomeric composite was also developed, applicable to long-term monitoring of microchannel pressure conditions.[4] Previously, we have demonstrated a microfluidic rheometer to characterize protein unfolding and aggregation in terms of a rheological aspect using a similar channel network of the microfluidic parallel circuit.[5]

[a)]Author to whom correspondence should be addressed. Electronic mail: jekyun@kaist.ac.kr. Tel.: +82-42-350-4315. FAX: +82-42-350-4310.

In this study, we integrate the previously reported channel network with various microfluidic channels for the measurement of hydraulic resistance of microchannels with complex fluid structure.

The hydraulic resistance of a channel being a measure of its opposition to the passage of a fluid flow is an important parameter for design of microfluidic devices that need to control the transport of fluid with high reliability and accuracy. The hydraulic resistance is constant for the given temperature and geometric condition, not depending on the amount of the fluid through and the pressure drop across the channel, particularly in the range of low Reynolds numbers in which most of microfluidic devices work.[6] Therefore, flow variables can be calculated even in complex microfluidic channel networks with the use of an equivalent electrical circuit model, in which each channel segment corresponds to an electrical resistor, and be used for design of microfluidic devices.[7–9] For instance, microfluidic networks for generation of concentration gradients commonly include channels of varying size in series and in parallel, branching, and recombining channels in such a way that flow branches into two or more separate channels and then come together again downstream, producing a desired concentration profile.[7,8] In these applications, hydraulic resistance is an important design parameter that determines whether the device principle works well. Consequently, any microfluidic applications that require a precise knowledge of flow profile and distribution will not be compromised without accurate measurement or calculation of hydraulic resistance.

The fluidic behavior in microchannels, especially in terms of channel friction (i.e., friction constant), has been investigated by comparing with conventional flow theories for macrochannels. Although early reports proposed the significant disparity between microfluidic flow behaviors and conventional theories, pointing out microscale effects as important causes for the deviation,[10–16] many recent researchers reported that there were no significant differences between micro- and macroscale flow behaviors. The latter claimed that the deviations might arise from issues of dead volumes in standard pressure measurement techniques, problems associated with interfacing microfluidic devices to standard pressure gauges, and measurement errors of channel dimension.[17–19] These limitations make it difficult to measure the hydraulic resistance of microfluidic components in microscales with high reliability and accuracy.

Herein we propose a microfluidic method that overcomes the above limitations and demonstrate its ability to measure an unknown hydraulic resistance and its friction constant without any external measurement setup by balancing two parallel channels with a common pressure drop, one channel of which has an unknown resistance.

II. MATERIALS AND METHOD

A. Design and fabrication of a microfluidic parallel circuit

The microfluidic parallel circuit was fabricated in poly(dimethylsiloxane) (PDMS) using soft lithography. A mold was obtained by patterning a SU-8 photoresist (Microchem Corp., MA) on a silicon wafer by standard photolithography. PDMS was cast on the mold and cured for 3 h in a convection oven at 65 °C for complete cross-linking. The PDMS channel was sealed with a glass slide after exposure to oxygen plasma for 30 s. The channel dimensions were measured with a surface profiler (Alpha-step 500; KLA-Tencor Corp., CA); the height was 27.1 ± 0.2 μm.

B. Sample preparation

All aqueous solutions were prepared with de-ionized water from the Milli-Q filtration system (Millipore Co., MA). Blood samples were obtained from the Republic of Korea National Red Cross Organization (Daejeon, Korea) in compliance with safety regulations.

C. Experimental setup

The microchannels were imaged with a microscope (TS100; Nikon Co.,) equipped with a charge-coupled device (DS-2MBWc; Nikon Co.). Two syringe pumps (KDS100; KD Scientific Inc., Holliston, MA) with pumping accuracy of less than 1% were used to produce 0.6–20.0 ml/h

flows through the microchannels. A commercial image analyzing program, i-Solution (IMT i-solution Inc., Korea), was used to measure the fluid interface in the microchannels. The program measures the lines drawn by users and converts their pixel information into metric information. Each pixel from the acquired images represents $\approx 1.1\ \mu$m.

D. Computational fluid dynamics simulation

Simulations of the pressure and velocity fields in the microchannels were performed with a commercial computational fluid dynamics (CFD) solver (CFD-ACE+; ESI Group., Huntsville, AL).

III. RESULTS AND DISCUSSION

From the electronic-hydraulic analogy, the laminar incompressible flow of steady state inside a channel is described by[6]

$$Q = \frac{\Delta P}{R}, \tag{1}$$

where Q is the volumetric flow rate, ΔP is the pressure drop from one end of the channel to the other, and R is the hydraulic resistance of the channel. A channel of uniform cross-section has a resistance proportional to its length (L), the viscosity (μ) of a fluid, the friction factor (f) of the channel, and Reynolds number (Re); it is inversely proportional both to its cross-sectional area (A) and the square of its hydraulic diameter (D_h), given by[6]

$$R = (f\ \mathrm{Re})\frac{\mu L}{2D_h^2 A}. \tag{2}$$

The hydraulic resistance (R) is constant for the given temperature and geometric condition, particularly in the range of low Re in which most of microfluidic devices work. However, additional pressure losses due to turbulence should be addressed for calculation of hydraulic resistance in the range of high Re in which inertial effects begin to dominate. Figure 1 shows a schematic of a microfluidic parallel circuit and its principle to measure an unknown hydraulic resistance without any measurement setup. Its operational principle is similar to the potentiometer or the Wheatstone bridge. Instead of comparing the electric potential, the volumetric flow rate (Q_1) through the channel with the unknown resistance to be measured is adjusted until two colored flows separately branch into two parallel channels, thereby providing information concerning the volumetric flow rate through each channel. In the parallel configuration, the same pressure drop ($\Delta P = P_1 - P_2$) across the channel ends is applicable to all channel components connected in parallel. Therefore, if Q_1, Q_2, and R_{ref} are known, then R_x can be defined as

$$R_x = R_{ref}\frac{Q_2}{Q_1}. \tag{3}$$

The friction factor (f) is a dimensionless quantity used in the Darcy–Weisbach equation, for description of frictional losses in internal flow as well as open channel flow and linearly varies as 1/Re in the range of low Reynolds numbers. The friction constant (f Re) defined as the product of f and Re is constant in the range of low Re. In solving Eqs. (2) and (3), the friction constant for the unknown resistance, $(f\ \mathrm{Re})_x$ is given by the following formula:

$$(f\ \mathrm{Re})_x = (f\ \mathrm{Re})_{ref}\frac{\mu_2}{\mu_1}\left(\frac{(D_h)_x^2 A_x}{(D_h)_{ref}^2 A_{ref}}\right)\frac{Q_2}{Q_1}, \tag{4}$$

where $(f\ \mathrm{Re})_{ref}$ is the friction constant of the reference channel, μ is the fluid viscosity, and A is the cross-sectional area of the channel. D_h is the hydraulic diameter, defined as $2wh/(w+h)$, where w and h are the width and height of the channel, respectively. Therefore, if the dimensions of the

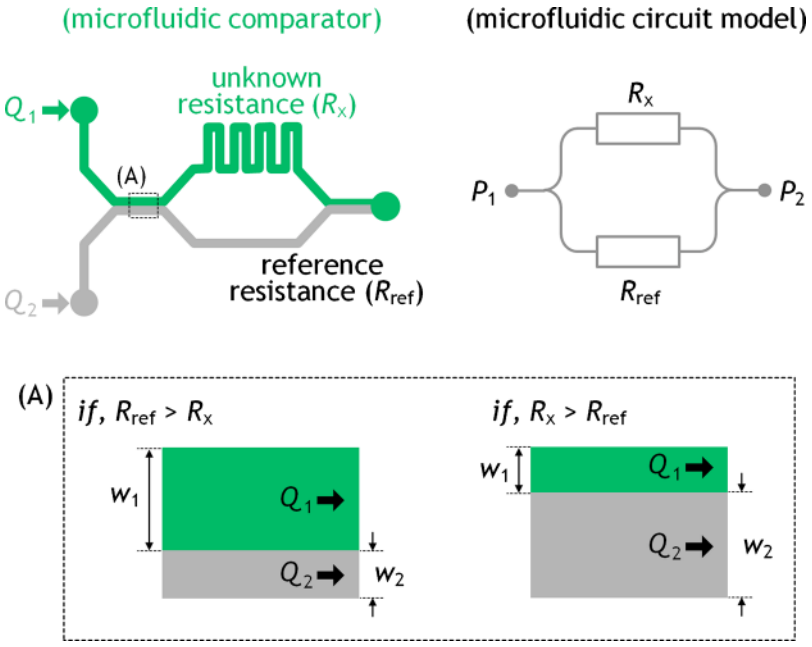

FIG. 1. Schematic of the microfluidic parallel circuit consisting of two channels connected in parallel, one channel of which has an unknown hydraulic resistance (R_x). In the parallel microfluidic circuit, the pressure drop ($\Delta P = P_1 - P_2$) across each channel is the same, and the total volume of fluid through the circuit is the sum of the volumes through all the components by mass conservation. The flow volume through each channel is found by adjusting feeding rates of two different fluids, one of which is colored with a dye. Therefore, if R_{ref} is known, then R_x can be measured simply by solving a proportional equation in terms of volumetric flow rate and hydraulic resistance. The area (A) denotes the comparison region to measure the flow distribution.

channel, the fluid viscosity, and $(f\ \mathrm{Re})_{ref}$ are known to high precision, then $(f\ \mathrm{Re})_x$ can be measured to high precision.

We demonstrated the proper functioning of the microfluidic parallel circuit for measurement of hydraulic resistance that contains a reference channel with a fixed width of 115 μm and a test channel as an unknown resistance with varying widths from 40 to 232 μm (Fig. 2). The measurements were obtained with aqueous streams colored with red food dye and performed at room temperature. Figure 3 presents the evolution of the interface between two colored flows that separately branch into two parallel, downstream channels, as shown in the insets of Fig. 2. The feeding rate of the fluid through the test channel was adjusted from 0.6 to 4.1 ml/h, while the feeding rate through the reference channel was fixed at 2.0 ml/h. The flow ratio, Q_1/Q_2 or w_1/w_2, linearly grows as the width of the test channel increases. The velocity profile across the channel width tends toward a pluglike form, analogous to the electro-osmotic flow profile as the aspect ratio of the channel cross-section is decreased.[20] Due to the low aspect ratio of 0.06 for the comparison region, its velocity profile can be "pluglike" across the channel width. Therefore, the ratio of the flow rate, Q_1/Q_2 is the same with the ratio of the widths of two colored flows, w_1/w_2, in the comparison region. The position of the interface between the two fluids did not move when the flow rates were increased, while the ratio between them is kept constant.

By using the raw data obtained from Fig. 3(b), calculations of the friction factor were performed by Eq. (4) and compared to the numerical simulations. The Darcy friction factor (f_D) is defined as[19]

$$f_D = \frac{2D_h}{\rho u^2}\frac{\Delta P}{L}, \tag{5}$$

where ρ is the fluid density and u is the average fluid velocity. The friction constant, $(f\ \mathrm{Re})_D$, can be expressed as the product of f and Re, where Re is defined as $D_h \rho u/\mu$,

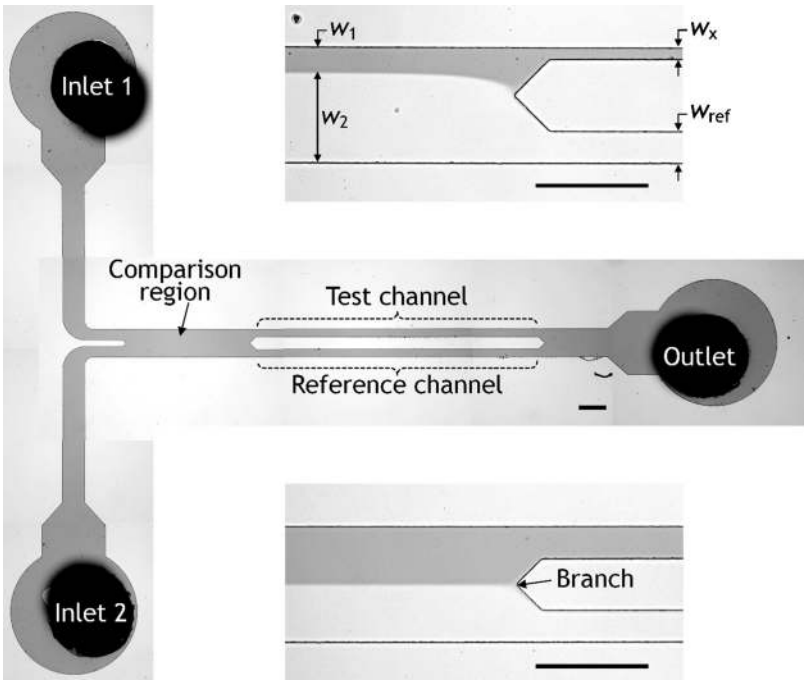

FIG. 2. Optical micrograph showing a microfluidic parallel circuit consisting of two inlets, a comparison region, test and reference channels connected in parallel, and an outlet. The width of the test channel (w_x) as an unknown resistance is varied from 40 to 232 μm, while the width of the reference channel (w_{ref}) is fixed at 115 μm. The widths of the test channels (w_x) are 40 and 115 μm for the upper and lower insets, respectively. In the insets, two different fluids, one of which is colored with a dye, are completely separated at the branch, thereby providing information concerning the volumetric flow rate through each channel (scale bars of 400 μm).

$$(f\ \mathrm{Re})_D = \frac{2D_h^2}{\mu u}\frac{\Delta P}{L}. \tag{6}$$

The pressure drops and fluid velocities across the microchannels were acquired by using a commercial CFD solver; thereby numerical data for the friction constant were calculated by Eq. (6). Since the friction constant for the reference channel is not available due to the above-mentioned problems, such as dead volumes in standard pressure measurement techniques and difficulty of interfacing between microchannels to standard pressure gauges, we used the numerical friction

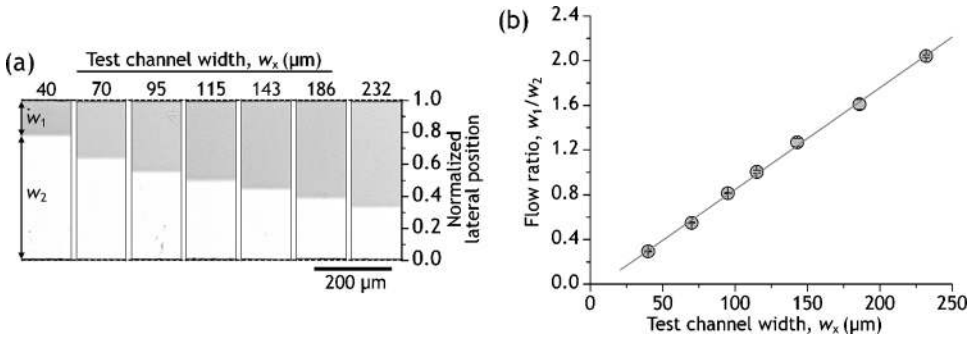

FIG. 3. Operation of the microfluidic parallel circuit. (a) Optical micrographs showing variation of the flow ratio between w_1 and w_2 in the comparison region as a function of the test channel width (w_x), while the width of the reference channel (w_{ref}) is fixed at 115 μm. (b) Measured flow ratio between w_1 and w_2 vs the width of the test channel (w_x). The line is a linear fit to the data; its slope is 0.0091/μm and R^2=0.9988.

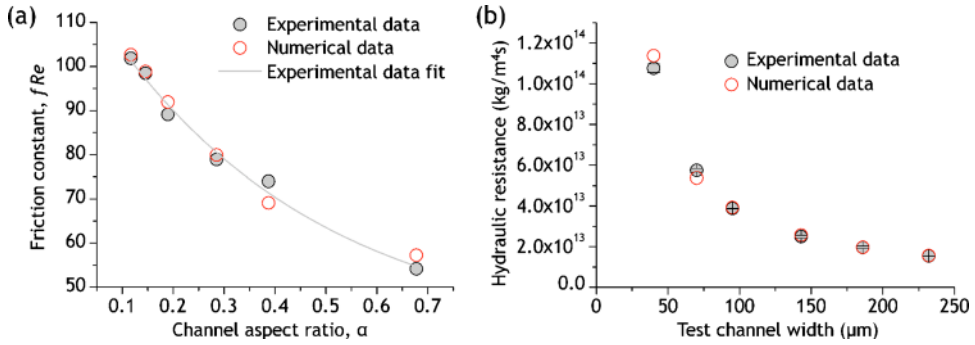

FIG. 4. Comparison of experimental data for friction constant and hydraulic resistance with numerical data. (a) Plot of the friction constant vs the aspect ratio of the channel cross-section. (b) Plot of the hydraulic resistance vs the width of the test channel.

constants of 84.2 and corresponding hydrodynamic resistance of 3.16×10^{13} kg/m^4 as reference for the reference channel of 115 μm in width. Figure 4 shows the comparison of friction constants and hydraulic resistances between experimental and numerical data. It is shown that the experimental results are in good agreement with the numerical data. The hydraulic resistances were then calculated by multiplying the friction constants with the corresponding channel dimensions using Eq. (2). The measured hydraulic resistance exponentially decreases as the width of the test channel increases and closely overlays the numerical data, as shown in Fig. 4(b). The calculated values of hydraulic resistance are 10.77 ± 0.21, 5.75 ± 0.08, 3.88 ± 0.02, 2.49 ± 0.07, 1.96 ± 0.06, and $1.55\pm0.01\times10^{13}$ kg/m^4 s for the widths of the test channel of 40, 70, 95, 143, 186, and 232, respectively. The difference between the experimental and theoretical data is small, but increased as the width of the test channel is decreased (Fig. 4). In order to explain this discrepancy, several microscale effects that can affect the fluid flow in microchannels should be discussed. First, the entrance effect can result in the increased friction constant. In the channel entrance, the boundary layer develops from a thin initial shear layer to fully developed Poiseuille flows within a short entrance length. Due to this frictional transition, the friction factor in the entrance region is always larger than that of fully developed flow. This entrance effect is significant when the dimensionless hydrodynamic length, $L/(D_h\ \mathrm{Re})$, is larger than 0.1.[11] However, the hydrodynamic entrance effect on the flow friction in this experiment can be ignored due to the high dimensionless hydrodynamic length of 11.7 in the reference channel. Second, viscous dissipation effect on the friction factor should be considered. Viscous dissipation represents an increase in internal energy due to the mechanical work done on a fluid by viscous forces. This viscous heating is significant for microchannels with $D_h<100$ μm and its effects on the local viscosity and friction factor increase as the aspect ratio of the channel cross-section deviates from unity.[10] However, this microscale effect is also negligible because the channel length of 4.5 mm is too short to change the fluid temperature by viscous dissipation.[13] In addition, the deviation can result from actual channel dimensions and channel roughness. Although further studies will be required to explain the discrepancy between the experimental and theoretical data, these experimental results are readily applicable to the design of microfluidic devices due to direct comparison of the test channels with the reference channel. This microfluidic comparison is conducted totally in microenvironments and excludes the above-mentioned errors that can arise from issues of dead volumes in standard pressure measurement techniques and problems associated with interfacing microfluidic devices to standard pressure gauges. Therefore, experimental results obtained from this method can be useful to exactly tailor or diagnose flow distributions in microfluidic networks.

The hydrodynamic resistance is determined by the liquid properties, channel dimensions, and channel roughness. The variation of surface property can have an influence on the measurement results only at low shear rates below 10 s^{-1} due to the wall-slip and electroviscous effect.[21] At the current operational condition over 100 s^{-1}, the effect of the surface property on the measurement results is negligible.

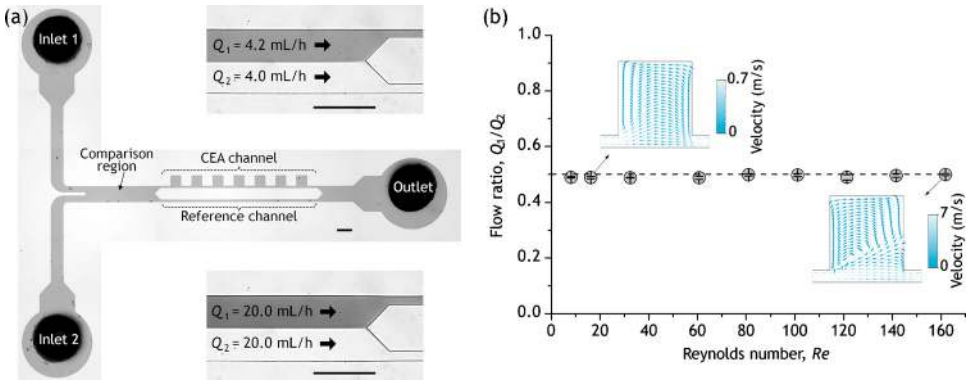

FIG. 5. Measurement of the hydraulic resistance of the CEA channel. (a) Optical micrograph showing a microfluidic parallel circuit consisting of two inlets, a comparison region, the CEA channel as a test channel and reference channel connected in parallel, and an outlet. The width of the reference channel (w_{ref}) is fixed at 60 μm. The CEA channel has a connected structure of a contraction region of 50 μm wide and 300 μm long, and an expansion region of 350 μm wide and 300 μm long. The insets show balancing two different fluids at the branch (scale bars of 400 μm). (b) Flow ratios between Q_1 and Q_2 as a function of Re in the CEA channel. The dashed line denotes the flow ratio of 1.0. The insets display flow patterns in the expansion regions. At Re of 161.9, the expansion vortex by flow separation occupies the expansion region.

Microfluidic applications are often accompanied by channels of complex geometry that vary in width and height. However, many research efforts to measure friction constant have been done in flows of straight channels, while experimental investigations of flows in microchannels of complex geometry is insufficient to predict the fluid transport in such channels with high accuracy. In addition, it is more practical to define an equivalent resistance of such complex channels rather than to describe their loss coefficients for designing the fluid distribution in microchannels. To demonstrate the ability of the microfluidic parallel circuit to measure a resistance of a channel of complex geometry, we fabricated a contraction–expansion array (CEA) microchannel with repeated patterns of a sudden contraction (50 μm wide and 300 μm long) and expansion (350 μm wide and 300 μm long) in the microfluidic parallel circuit [Fig. 5(a)]. The CEA channel and the reference channel with a width of 60 μm are connected in parallel. The feeding rates through the channels were obtained when the colored aqueous streams separately branch into two parallel channels, as shown in the insets of Fig. 5(a). The feeding rate of the fluid through each channel was varied from 1.0 to 20.0 ml/h that corresponds to Re of 8.1–161.9 in the CEA channel. Over the range of the flow rate, the measured flow ratios, Q_1/Q_2, were 1.03 ± 0.02 [Fig. 5(b)]. The unity means that the resistance of the CEA microchannel is equivalent to that of the reference channel. From Fig. 4(b), the hydraulic resistance of the reference channel (60 μm in width) is found to be 6.96×10^{13} kg/m^4 s. The hydraulic resistance of the CEA microchannel is equivalent to 6.96×10^{13} kg/m^4 s. Although this experiment exploits the reference channel with the fixed hydraulic resistance, tunable fluidic resistors can be used to obtain the equivalent linear channel of a test channel of complex geometry.[22] The resistance of the tunable fluidic resistors as a reference can be adjusted until the flow ratio becomes unity, then the equivalent hydraulic resistance of a test channel can be measured. The abrupt change of the channel cross-section causes the flow to have strong radial velocity components that can increase the turbulence kinetic energy and induce an early laminar-to-turbulent transition at relatively low Re.[23] However, interestingly, we did not observe any deviation of the flow ratio from unity as increasing Re, thereby developing the expansion vortex, as shown in the lower inset of Fig. 5(b). This might be attributed to the low Re of 161.9. For laminar pipe flow, $\mathrm{Re} < 2300$, the friction constant can be estimated as constant.[10] In the same context, for the microflow, $\mathrm{Re} \leq 162$, the friction constant can be estimated as constant. However, further studies will be required to explain more details about maintaining the flow ratio to unity regardless of Re.

In order to investigate the effect of the fluid viscosity on the operation of the microfluidic

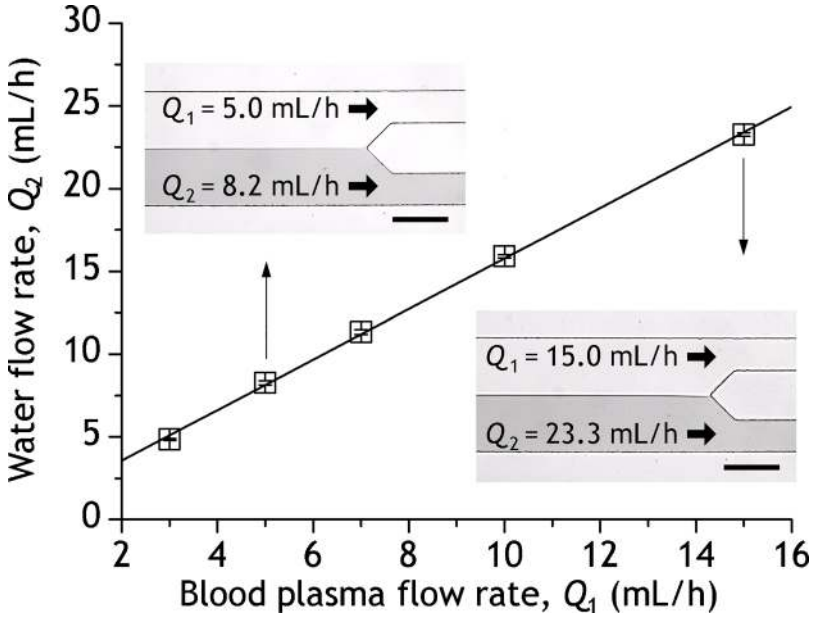

FIG. 6. Effect of the fluid viscosity on the operation of the microfluidic parallel circuit. The flow ratio between Q_1 and Q_2 for balancing is constant for specific viscosity independently of the increase of the flow rate. The lines are the linear fits to the data; the slope is 1.52 and R^2=0.99. The insets show balancing two fluids with different viscosities at the branch. The upper and lower parts of fluid streams denote fluid streams of blood plasma and an aqueous solution (water), respectively (scale bars of 200 μm).

parallel circuit, we injected human blood plasma and an aqueous solution (water) to the microfluidic parallel circuit consisting of the test and resistance channels with the same width of 115 μm. The hydraulic resistance of a channel in the range of low Re depends on its geometric parameters, such as the aspect ratio of its cross-section rather than other fluidic properties, such as flow rate. Therefore, at a given pressure drop between channel ends, the flow rate through a microchannel only depends on the fluid viscosity and is linearly decreased as the fluid becomes more viscous.[5] From this relationship, we can calculate the viscosity of blood if the fluid viscosity and feeding rates through the reference channel and the test channel are known, as the following formula:[5]

$$\mu_1 = \mu_2 \frac{Q_2}{Q_1}. \tag{7}$$

The feeding rate of the aqueous solution is higher than that of blood plasma that has a higher viscosity as two fluid streams separately branch into two parallel channels, as shown in the insets of Fig. 6. The calculated viscosity is 1.34 cP for blood plasma with the measured flow ratio, Q_2/Q_1=1.52, and water viscosity at 25°, μ_2=0.88 cP.[24] The viscosity of blood plasma is in good agreement with the value of 1.24 cP found in literature.[25] This result supports that the microfluidic parallel circuit well reflects the change of hydraulic resistance by internal-flow properties, such as viscosity as well as channel geometry.

IV. CONCLUSION

In this paper, we introduced a microfluidic method to measure the friction constant and hydraulic resistance of a microfluidic channel without any measurement setup, such as standard pressure gauges, by directly comparing the test channel of an unknown resistance with the reference channel with a known resistance. Additionally, this work demonstrates a solution to the challenging problem of resistance measurement without precise measurement setups, such as

standard pressure gauges. With this method, we defined an equivalent linear channel of the CEA microchannel with repeated patterns of a sudden contraction and expansion. This approach to define a channel segment with complex patterns will be practical for design of microchannel networks that an equivalent electrical circuit model is commonly used. Most importantly, this method will be helpful to develop modular microfluidic systems[26,27] that require precise characterization of each channel module. As a means to characterize the newly developed channel segment with predefined standard channels, this method can provide practical design parameters that facilitate design of microfluidic networks.

ACKNOWLEDGMENTS

This research was supported by the National Research Laboratory (NRL) Program grant (No. R0A-2008-000-20109-0), by the Nano/Bio Science and Technology Program grant (No. 2008-00771), and by the Converging Research Center Program grant (No. 2009-0093663) through the National Research Foundation of Korea (NRF) funded by the Ministry of Education, Science and Technology (MEST).

[1] M. Abkarian, M. Faivre, and H. A. Stone, Proc. Natl. Acad. Sci. U.S.A. **103**, 538 (2006).
[2] S. A. Vanapalli, A. G. Banpurkar, D. van den Ende, M. H. G. Duits, and F. Mugele, Lab Chip **9**, 982 (2009).
[3] V. Labrot, M. Schindler, P. Guillot, A. Colin, and M. Joanicot, Biomicrofluidics **3**, 012804 (2009).
[4] L. Wang, M. Zhang, M. Yang, W. Zhu, J. Wu, X. Gong, and W. Wen, Biomicrofluidics **3**, 034105 (2009).
[5] S. Choi and J.-K. Park, Small **6**, 1306 (2010).
[6] A. Akers, M. Gassman, and R. Smith, *Hydraulic Power System Analysis* (CRC, Florida, 2006).
[7] K. Lee, C. Kim, B. Ahn, R. Panchapakesan, A. R. Full, L. Nordee, J. Y. Kang, and K. W. Oh, Lab Chip **9**, 709 (2009).
[8] K. Hattori, S. Sugiura, and T. Kanamori, Lab Chip **9**, 1763 (2009).
[9] D. Kim, N. C. Chesler, and D. J. Beebe, Lab Chip **6**, 639 (2006).
[10] J. Koo and C. Kleinstreuer, J. Micromech. Microeng. **13**, 568 (2003).
[11] G. Gamrat, M. Favre-Marinet, and D. Asendrych, Int. J. Heat Mass Transfer **48**, 2943 (2005).
[12] D. Brutin and L. Tadrist, Phys. Fluids **15**, 653 (2003).
[13] B. Xu, K. T. Ooi, C. Mavriplis, and M. E. Zaghloul, J. Micromech. Microeng. **13**, 53 (2003).
[14] S. M. Ghiaasiaan and T. S. Laker, Int. J. Heat Mass Transfer **44**, 2777 (2001).
[15] M. S. El-Genk and I.-H. Yang, J. Heat Transfer **130**, 082405 (2008).
[16] H. Y. Wu and P. Cheng, Int. J. Heat Mass Transfer **46**, 2519 (2003).
[17] M. J. Kohl, S. I. Abdel-Khalik, S. M. Jeter, and D. L. Sadowski, Sens. Actuators, A **118**, 212 (2005).
[18] J. Judy, D. Maynes, and B. W. Webb, Int. J. Heat Mass Transfer **45**, 3477 (2002).
[19] B. Xu, K. T. Ooi, N. T. Wong, and W. K. Choi, Int. Commun. Heat Mass Transfer **27**, 1165 (2000).
[20] G.-B. Lee, C.-C. Chang, S.-B. Huang, and R.-J. Yang, J. Micromech. Microeng. **16**, 1024 (2006).
[21] P. Guillot, P. Panizza, J.-B. Salmon, M. Joanicot, and A. Colin, Langmuir **22**, 6438 (2006).
[22] E. W. Lam, G. A. Cooksey, B. A. Finlayson, and A. Folch, Appl. Phys. Lett. **89**, 164105 (2006).
[23] M. G. Lee, S. Choi, and J.-K. Park, Appl. Phys. Lett. **95**, 051902 (2009).
[24] W. Hirst and R. A. Cox, Biochem. J. **159**, 259 (1976).
[25] U. Windberger, A. Bartholovitsch, R. Plasenzotti, K. J. Korak, and G. Heinze, Exp. Physiol. **88**, 431 (2003).
[26] K. A. Shaikh, K. S. Ryu, E. D. Goluch, J.-M. Nam, J. Liu, C. S. Thaxton, T. N. Chiesl, A. E. Barron, Y. Lu, C. A. Mirkin, and C. Liu, Proc. Natl. Acad. Sci. U.S.A. **102**, 9745 (2005).
[27] M. Rhee and M. A. Burns, Lab Chip **8**, 1365 (2008).